Osteoarthritis and Cartilage 27 (2019) 1347–1360

Osteoarthritis and Cartilage

Modulation of the Wnt pathway through inhibition of CLK2 and DYRK1A by lorecivivint as a novel, potentially disease-modifying approach for knee osteoarthritis treatment

V. Deshmukh †, A.L. O'Green † [a], C. Bossard † [a], T. Seo †, L. Lamangan †, M. Ibanez †, A. Ghias †, C. Lai †, L. Do †, S. Cho †, J. Cahiwat †, K. Chiu †, M. Pedraza †, S. Anderson †, R. Harris †, L. Dellamary †, S. KC †, C. Barroga †, B. Melchior †, B. Tam ‡, S. Kennedy †, J. Tambiah †, J. Hood ‡, Y. Yazici † *

† *Samumed, LLC, San Diego, CA, USA*
‡ *Formerly Samumed, LLC, USA*

ARTICLE INFO

Article history:
Received 29 November 2018
Accepted 14 May 2019

Keywords:
Lorecivivint
SM04690
Osteoarthritis
Wnt pathway
CLK2
DYRK1A
Chondrocyte

SUMMARY

Objectives: Wnt pathway upregulation contributes to knee osteoarthritis (OA) through osteoblast differentiation, increased catabolic enzymes, and inflammation. The small-molecule Wnt pathway inhibitor, lorecivivint (SM04690), which previously demonstrated chondrogenesis and cartilage protection in an animal OA model, was evaluated to elucidate its mechanism of action.

Design: Biochemical assays measured kinase activity. Western blots measured protein phosphorylation in human mesenchymal stem cells (hMSCs), chondrocytes, and synovial fibroblasts. siRNA knockdown effects in hMSCs and BEAS-2B cells on Wnt pathway, chondrogenic genes, and LPS-induced inflammatory cytokines was measured by qPCR. *In vivo* anti-inflammation, pain, and function were evaluated following single intra-articular (IA) lorecivivint or vehicle injection in the monosodium iodoacetate (MIA)-induced rat OA model.

Results: Lorecivivint inhibited intranuclear kinases CDC-like kinase 2 (CLK2) and dual-specificity tyrosine phosphorylation-regulated kinase 1A (DYRK1A). Lorecivivint inhibited CLK2-mediated phosphorylation of serine/arginine-rich (SR) splicing factors and DYRK1A-mediated phosphorylation of SIRT1 and FOXO1. siRNA knockdowns identified a role for CLK2 and DYRK1A in Wnt pathway modulation without affecting β-catenin with CLK2 inhibition inducing early chondrogenesis and DYRK1A inhibition enhancing mature chondrocyte function. NF-κB and STAT3 inhibition by lorecivivint reduced inflammation. DYRK1A knockdown was sufficient for anti-inflammatory effects, while combined DYRK1A/CLK2 knockdown enhanced this effect. In the MIA model, lorecivivint inhibited production of inflammatory cytokines and cartilage degradative enzymes, resulting in increased joint cartilage, decreased pain, and improved weight-bearing function.

Conclusions: Lorecivivint inhibition of CLK2 and DYRK1A suggested a novel mechanism for Wnt pathway inhibition, enhancing chondrogenesis, chondrocyte function, and anti-inflammation. Lorecivivint shows potential to modify structure and improve symptoms of knee OA.

* Address correspondence and reprint requests to: Y. Yazici, Samumed LLC, 9381 Judicial Drive, Suite 160, San Diego, CA, 92121, USA. Tel: 1-858-926-2900.

E-mail addresses: vishal@samumed.com (V. Deshmukh), alyssao@samumed.com (A.L. O'Green), carine@samumed.com (C. Bossard), tims@samumed.com (T. Seo), lisa@samumed.com (L. Lamangan), maureen@samumed.com (M. Ibanez), abdullah@samumed.com (A. Ghias), carolyn@samumed.com (C. Lai), long@samumed.com (L. Do), shawn@samumed.com (S. Cho), joec@samumed.com (J. Cahiwat), kevin@samumed.com (K. Chiu), melinda@samumed.com (M. Pedraza), scotta@samumed.com (S. Anderson), rodney@samumed.com (R. Harris), luis@samumed.com (L. Dellamary), sunil@samumed.com (S. KC), charlene@samumed.com (C. Barroga), benoit@samumed.com (B. Melchior), byytam@sbcglobal.net (B. Tam), sarahk@samumed.com (S. Kennedy), jeymi@samumed.com (J. Tambiah), hoodpharmaceuticals@gmail.com (J. Hood), yusuf@samumed.com (Y. Yazici).

[a] equal contribution.

https://doi.org/10.1016/j.joca.2019.05.006

Introduction

Osteoarthritis (OA) affects approximately 30 million adults in the US and is a leading cause of disability worldwide[1]. OA is a whole joint disease, characterized by cartilage degradation, bony changes, and synovial inflammation, leading to joint space narrowing, pain, and loss of function[2]. While anti-inflammatory agents are broadly used in OA symptomatic treatment, these have not shown benefit in slowing structural progression, leaving surgical intervention as the only option. There is an unmet need for disease-modifying OA drugs (DMOAD) that benefit pain and function and mitigate the structural damage caused by OA. Approaches to DMOAD development include cartilage regeneration, inhibition of inflammation or cartilage catabolic enzymes, stimulating chondrocytes with growth factors, and restoring cartilage homeostasis[3–6].

The Wnt pathway is highly conserved across species and plays a central role in organogenesis, cell differentiation, and tissue remodeling[7]. Canonical Wnt signaling is initiated by Wnt proteins binding to frizzled (FZD) receptors, causing a breakdown of the cytoplasmic β-catenin destruction complex. Stabilized β-catenin translocates to the nucleus and interacts with T-cell factor/lymphoid enhancer factor (TCF/LEF) transcription factors to activate Wnt target gene expression[8]. Wnt signaling is tightly regulated at multiple levels, resulting in homeostatic signaling in most tissues. In the joint, homeostatic levels of Wnt signaling are essential for stem cell proliferation, chondrocyte differentiation, and function, with both β-catenin deletion and activation resulting in joint damage[9,10]. Wnt signaling is upregulated in OA joint tissues and drives bone differentiation, cartilage degradation, chondrocyte hypertrophy, and inflammation[11]. Given these central roles for Wnt signaling in OA pathogenesis, modulation of the Wnt pathway downstream of β-catenin offers a promising approach for homeostatic modulation of Wnt signaling and OA treatment.

Regulation of gene expression can be accomplished via several mechanisms including transcriptional control through phosphorylation of transcription factors and posttranscriptional regulation through alternative splicing. 95% of human genes are alternatively spliced[12], creating diversity of proteins from a single gene via inclusion or exclusion of introns and exons[13]. Splicing is regulated by various mechanisms including phosphorylation of pre-mRNA binding proteins such as the serine/arginine-rich splicing factors (SRSF)[13].

Lorecivivint, a potential DMOAD and small-molecule Wnt pathway inhibitor, has shown promising OA therapeutic effects, inducing chondrocyte differentiation, cartilage regeneration and protection, and improving joint health scores in a surgically induced joint destabilization (anterior cruciate ligament transection, partial medial meniscectomy; ACLT+pMMx) rat OA model[14]. In this report, the novel mechanism of action of lorecivivint, through inhibition of intranuclear kinases, is described for Wnt pathway modulation, chondrocyte differentiation, inhibition of cartilage degradation, and anti-inflammatory effects in OA models *in vitro* and *in vivo*.

Methods

Kinase assays

Lorecivivint (0.5 μM) was screened through 318 kinases (Thermo Fisher).

Cell culture and assays

Cell culture (Table S1), reporter, and chondrogenic assays performed as previously described[14].

Western blot, qPCR, and nanostring assays

Cells were treated as indicated, incubated at 37°C, 5% CO_2.

Total protein or nuclear/cytoplasmic fractions (NE-PER™, Thermo Fisher) were extracted. Western blot was performed as previously described[14] using primary and secondary antibodies (Table S2).

qPCR was performed using SYBR-green or TaqMan™ primers as previously described[14]. 50 ng RNA was hybridized with Tagsets and probe pools (nCounter® Vantage 3D™ Pathways, NanoString Technologies); gene counts measured using nCounter® SPRINT Profiler. Analysis described in Supplementary Methods.

siRNA knockdowns

Reverse transfections were performed with siRNA (GE Dharmacon, Table S3) using Lipofectamine RNAiMAX (Thermo Fisher).

In vivo animal model

The ACLT+pMMx model was performed and lorecivivint injected as previously described[14]. For the MIA model, rats (10 weeks old) were injected MIA (IA, 3 mg in 50 μl). IA lorecivivint (0.1 μg, 0.3 μg, 1 μg in 50 μl) or vehicle ($n = 10$ rats/group) was injected and knee joints were isolated for biochemical analysis or histology [Supplementary Fig. 22(a)]. Histology, OARSI scoring, qPCR, Nanostring, ELISA, and Western blot were performed as previously described[14]. Pain was measured using Von Frey apparatus (Harvard instruments) and weight distribution using Incapacitance meter (Stoelting, Inc).

Statistics and Additional Methods in Supplementary Methods.

Results

Novel intranuclear kinase targets: lorecivivint potently inhibited CLK2 and DYRK1A

Biochemical profiling using lorecivivint (0.5 μM) showed ≥90% inhibition of 7 kinases (out of 318) compared to DMSO. CLK2 was the most potently inhibited kinase ($IC_{50} = 5.8$ nM) with six other kinases showing $IC_{50s} \geq 90\%$ inhibition and within 15-fold of CLK2 IC_{50}. DYRK1A, within the same CMGC kinase group as the CLKs, showed $IC_{50} = 26.9$ nM. Overall, lorecivivint demonstrated selectivity against wild type kinases (≥90% inhibition or $IC_{50} \leq 100$ nM representing 2.5% of 318 kinases; Supplementary Fig. 1(a), Tables S4, S5).

Computational modeling of lorecivivint with CLK2 and DYRK1A identified multiple hydrogen-bond, donor–acceptor sites potentially driving lorecivivint activity. Lorecivivint docked to the ATP-binding sites of both kinases, forming hydrogen-bonds with GLU244, LEU246, and LYS193 in CLK2, and GLU239, LEU241, and LYS188 in DYRK1A [Supplementary Fig. 1(b)–(e)]. For CLK2, 100 out of 100 dockings landed within 2Å root-mean-square distance (RMSD; docking energy = −12.8 ± 2.0 kcal/mol) and for DYRK1A, 77 out of 100 dockings landed within 2Å RMSD (docking energy = −11.4 ± 2.0 kcal/mol). The predicted binding mode would completely block ATP binding, thus inhibiting the function of CLK2 and DYRK1A.

Novel intranuclear kinase targets: lorecivivint inhibited CLK- and DYRK1A-mediated signaling in hMSCs and chondrocytes

In vitro biochemical assays for CLK2 and DYRK1A confirmed potent lorecivivint inhibition of CLK2 (IC_{50} = 7.8 nM) and DYRK1A (IC_{50} = 26.9 nM) [Fig. 1(a)]. Compared to CLK2 inhibitors (CC-671, TG003, ML167, Leucettine L41, ML315)[15–19] and DYRK1A inhibitors (Harmine, EGCG, AZ191, ID-8, INDY, L41, ML315)[16,17,20–23] being developed for oncology or as tool compounds, lorecivivint was 2–300-fold more potent than other compounds [Supplementary Fig. 1(f) and (g)].

In human mesenchymal stem cells (hMSCs) and chondrocytes, CLK1, CLK2, CLK3, and DYRK1A were predominantly localized in the nucleus, while CLK4 was localized in the cytoplasm [Supplementary Fig. 1(h)]. CLKs exert their function by phosphorylating SRSF proteins[24,25]. The expression and phosphorylation of SRSF1, SRSF4, SRSF5, and SRSF6 were confirmed in hMSCs using specific siRNAs [Supplementary Fig. 2(a)–(g)]. No statistically significant changes in the expression of CLKs 1-4, DYRK1A, or SRSF4, SRSF5, and SRSF6 were observed in hMSCs or chondrocytes following WNT3A or CHIR99021 (GSK3β inhibitor) stimulation compared to unstimulated cells [Supplementary Fig. 1(i) and (j), 2(h), (i)].

Lorecivivint dose dependently inhibited the CLK-mediated phosphorylation of SRSF4, SRSF5, and SRSF6 in hMSCs and human chondrocytes [Fig. 1(b) and (c), Supplementary Fig. 3(a) and (b)] and was more potent than CC-671 (CLK2/TTK inhibitor), while Harmine (DYRK1A/B inhibitor) had no effects [Supplementary Fig. 3(c) and (d)]. Lorecivivint (30 nM) upregulated gene expression of CLKs 1-3 and downregulated SRSF4 and SRSF5 in hMSC and chondrocytes, while CLK4 was downregulated in hMSC and upregulated in chondrocytes [Supplementary Fig. 4(a) and (b)]. Spliceosome modulation by lorecivivint (30 nM, 100 nM) was shown by enlargement of nuclear speckles[25] in hMSCs and chondrocytes compared to DMSO [Fig. 1(d), Supplementary Fig. 4(c) and (d)]. CC-671 enlarged nuclear speckles at higher doses (10 μM, 3 μM), while Harmine had no effects [Supplementary Fig. 4(e) and (f)]. Treatment with lorecivivint also led to intron retention (IR) in the mRNA of several Wnt pathway genes [Supplementary Fig. 5(a) and (b)].

DYRK1A phosphorylates transcription factor FOXO1 and histone-modifying enzyme Sirtuin 1 (SIRT1)[26,27]. FOXO1 phosphorylation results in its exclusion from the nucleus and subsequent proteosomal degradation. Active nuclear FOXO1 has been shown to be involved in promoting chondrocyte homeostasis, stress response, proteoglycan (PRG4) production, and protection from OA development[28,29]. Lorecivivint dose dependently inhibited the phosphorylation of FOXO1 in chondrocytes in the presence of OA-related inflammatory cytokine IL-1β with corresponding increases in total FOXO1 protein levels and nuclear localization compared to DMSO [Fig. 1(e) and (f), Supplementary Fig. 6(a) and (b)]. Lorecivivint also dose dependently and more potently inhibited phosphorylation of SIRT1 (pSer27, pSer47) in hMSCs and chondrocytes in the presence of IL-1β, compared to DMSO and Harmine, while CC-671 had no effects [Fig. 1(g), Supplementary Fig. 6(c) and (d)]. Lorecivivint (30 nM) did not affect *FOXO1*, *SIRT1,* or *DYRK1A* gene expression [Supplementary Fig. 6(e)–(g)], indicating that lorecivivint effects on these proteins were predominantly at the posttranslational level.

Wnt pathway inhibition: inhibition of CLK2 and DYRK1A inhibited the Wnt pathway in hMSCs

In hMSCs, CLK2 or DYRK1A knockdowns inhibited Wnt pathway gene expression (*AXIN2*, *TCF7*, and *TCF4*) while small increases were observed in β-catenin (*CTNNB1)* expression, compared to non-targeted siRNA control (siCtrl; Fig. 2(a) and (b)), consistent with lorecivivint inhibitory effects [Supplementary Fig. 8(b)]. Further, no decrease in active and total β-catenin levels were observed with lorecivivint treatment in WNT3A- and CHIR-stimulated hMSCs, chondrocytes, and 293T cells [Supplementary Fig. 7(a) and (b), Supplementary Fig. 8(a)]. CC-671 and Harmine inhibited the TCF/LEF reporter in SW480 cells at 20–200-fold less potency than lorecivivint, while HIPK2 inhibitors A64 and TBID had no effects [Supplementary Fig. 8(c)]. CC-671 inhibited expression of *AXIN2, TCF7, LEF1,* and *TCF4* in CHIR99021-stimulated and unstimulated hMSCs, while Harmine inhibited *AXIN2, LEF1,* and *TCF4* [Supplementary Fig. 8(d) and (e)].

Knockdowns of CLK2, DYRK1A, and CLK2+DYRK1A decreased the expression of 47, 37, and 69 genes and upregulated 21, 29, and 37 genes, respectively, (Nanostring's nCounter® Vantage 3D™ Wnt Pathways panel; >1.5-fold change, FDR-adjusted, $q < 0.05$) compared to siCtrl, while lorecivivint downregulated 80 genes and upregulated 47 genes [Fig. 2(c), Supplementary Fig. 9(a)–(f)]. Downregulation of *AXIN2, TCF7, LRP5, BAMBI, NKD1, PAI-1, LRP6, FZD6, FZD7*, *PITX2*, *ERBB2*, and *CTGF* gene expression and increased levels of Wnt pathway inhibitors *SFRP2* and *DACT1* were confirmed by qPCR [Fig. 2(d) and (e)]. In contrast, β-catenin knockdown downregulated 38 genes and upregulated 6 genes [Supplementary Fig. 9(e)].

Although lorecivivint also inhibited HIPK2 kinase (IC_{50} = 16.8 nM), HIPK2 knockdowns in hMSCs showed small but significant increases in gene expression of *AXIN2, TCF7,* and *TCF4* compared to siCtrl [Supplementary Fig. 9(g)–(i)], consistent with the role of HIPK2 in repressing Wnt signaling[30].

Wnt pathway inhibition and chondrogenesis: inhibition of TCF7 induced chondrocyte differentiation in hMSCs

Knockdowns of β-catenin, TCF7, LEF1, and TCF4 in hMSCs [Supplementary Fig. 10(a)–(h)] led to inhibition of Wnt signaling, demonstrated by decreased *AXIN2, TCF7, LEF1,* and *TCF4* expression [Supplementary Fig. 10(i)–(m)]. However, β-catenin, LEF1, and TCF4 knockdowns did not induce chondrocyte formation in hMSCs, measured by *COMP*, *SOX9,* and *RUNX1* gene expression. Consistent with the role of activated Wnt signaling in bone differentiation, osteoblast promoting factor *RUNX2* was decreased with β-catenin, LEF1, and TCF4 knockdowns compared to siCtrl [Fig. 3(a) and (b)].

TCF7 knockdown resulted in 30-fold increased *COMP* expression, small but significantly increased (1.5–2-fold, $p < 0.05$) *SOX9* and *RUNX1* expression, and decreased *RUNX2* expression compared to siCtrl [Fig. 3(c) and (d)], and these results were comparable to lorecivivint or TGF-β3 treatment of hMSCs [Fig. 4(a)–(f)]. Early chondrogenic differentiation in 10-day hMSC cultures stained with Rhodamine B showed chondrogenic nodules with TCF7 knockdown, but not with β-catenin, LEF1, and TCF4 knockdowns [Fig. 3(e) and (f)]. TCF7 knockdown did not significantly change the expression levels of *CLK2* and *DYRK1A* compared to siCtrl [Supplementary Fig. 10 (n,o)].

Cartilage Regeneration: CLK2 Inhibition induced early chondrocyte differentiation in hMSCs and DYRK1A inhibition enhanced differentiated chondrocyte function

CLK2 knockdown in hMSCs [Supplementary Fig. 11(a) and (b)] increased early chondrocyte differentiation with 50-fold increased *COMP* and 3–4-fold increased *SOX9* and *RUNX1* expression compared to siCtrl. These changes were similar to TGF-β3 or lorecivivint treatment [Fig. 4(a)–(f), Supplementary Fig. 11(c)–(e)]. CLK1 and CLK4 knockdowns induced small but significantly increased (4–6-fold, $p < 0.05$) *COMP* expression. CLK1 knockdown induced 1.5-fold increased *SOX9* expression while CLK3 or DYRK1A

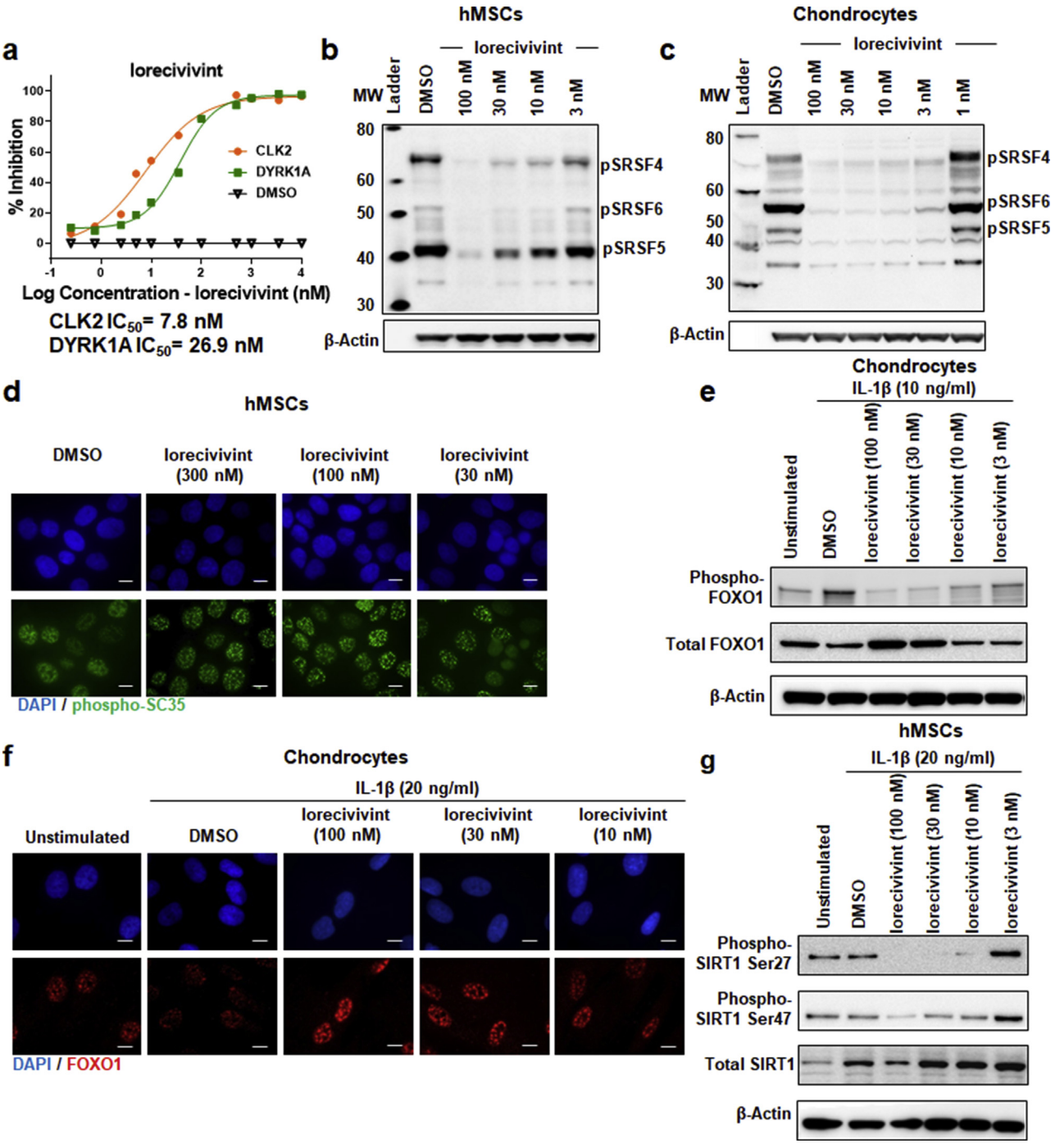

Fig. 1. Lorecivivint (SM04690) was a potent inhibitor of CLKs and DYRK1A. **(a)** Dose response for *in vitro* biochemical inhibition of CLK2 and DYRK1A by lorecivivint ($n = 4$). **(b, c)** Western blot of phospho-SRSF in **(b)** human mesenchymal stem cells (hMSCs) and **(c)** human chondrocytes following treatment with lorecivivint or DMSO for 1 hr. **(d)** Representative immunofluorescence images of hMSCs treated with lorecivivint or DMSO for 6 hrs. Cells were stained with phospho-SC35 antibody (green) or DAPI nuclear stain (blue). **(e)** Western blot of phospho- and total FOXO1 in human chondrocytes following treatment with IL-1β and lorecivivint or DMSO for 72 hrs. **(f)** Representative immunofluorescence images of human chondrocytes treated with IL-1β and lorecivivint or DMSO for 72 hrs. Cells were stained with anti-FOXO1 antibody (red) and DAPI nuclear stain (blue) **(g)** Western blot of phospho-SIRT1 (Ser27 and Ser47) and total SIRT1 in hMSCs following treatment with IL-1β and lorecivivint or DMSO for 24 hrs. All scale bars, 10 μm. β-actin serves as a loading control for Western blots. Data representative of at least 3 independent experiments.

knockdowns had no significant effects on *COMP*, *SOX9*, and *RUNX1* expression compared to siCtrl [Supplementary Fig. 11(f)–(h)]. No significant changes were observed in *RUNX2* expression with any knockdown [Supplementary Fig. 11(i)].

CC-671 induced chondrocyte differentiation at 100-fold less potency than lorecivivint, consistent with its less potent CLK2 inhibition *in vitro*, while Harmine had no effects [Supplementary Fig. 11(j)], consistent with the lack of early chondrocyte

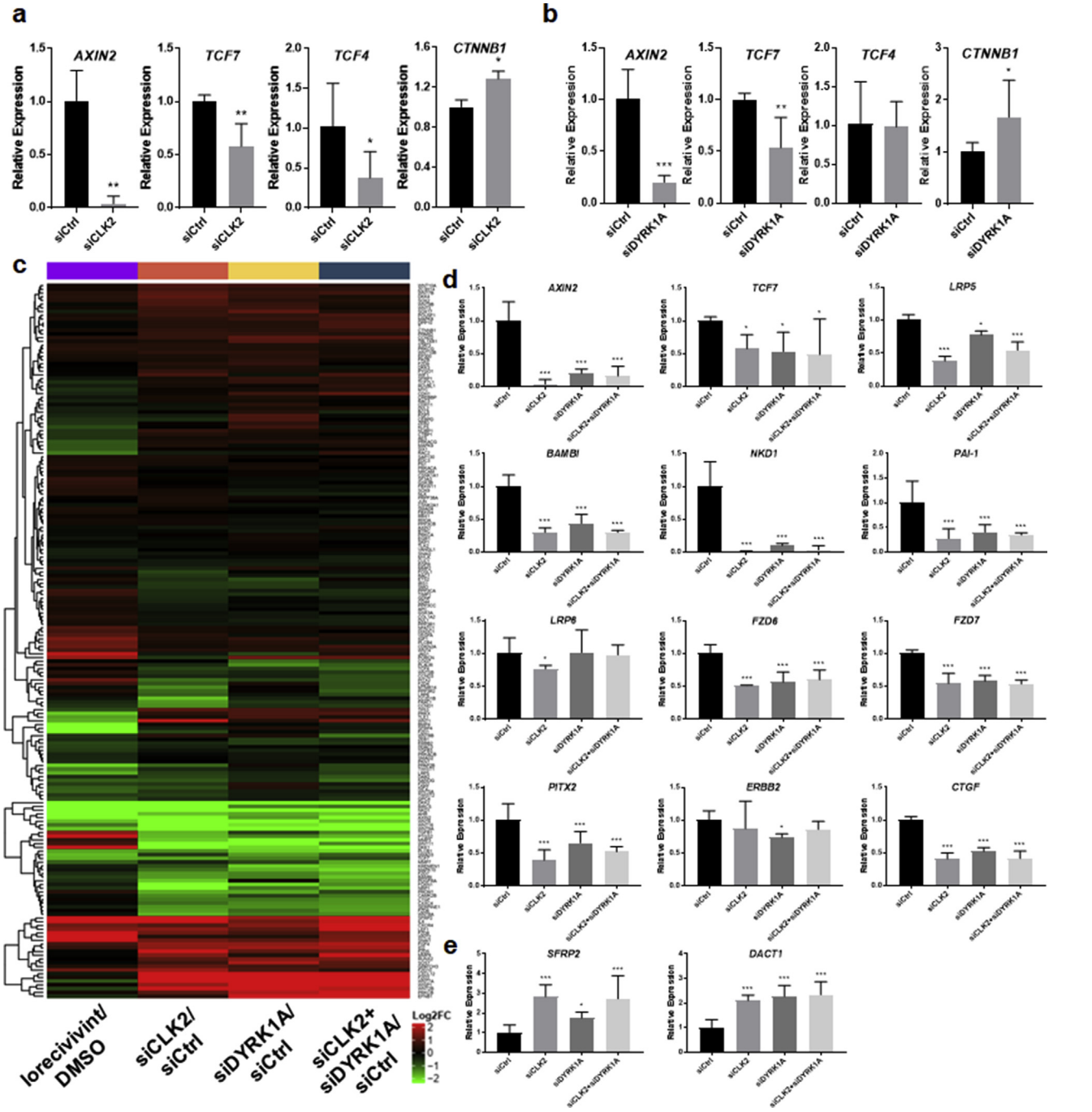

Fig. 2. Inhibition of CLK2 and DYRK1A inhibited the Wnt pathway. **(a, b)** Gene expression of Wnt pathway markers *AXIN2, TCF7, TCF4,* and *CTNNB1* in hMSCs at 72 hrs following treatment with either non-targeted control siRNA or siRNA specific to **(a)** CLK2 or **(b)** DYRK1A. Fold change relative to siRNA control ($n = 3$, Mean ± 95% CI, $^{*}p < 0.05$, $^{**}p < 0.01$, $^{***}p < 0.01$, *t*-test). **(c)** Effects of treatment of hMSCs with siRNA specific to CLK2, DYRK1A, CLK2+DYRK1A, non-targeted control siRNA, DMSO, and lorecivivint on Wnt pathway gene expression at 72 hrs following treatment, measured using the Nanostring nCounter® gene array. **(d, e)** Confirmation of gene expression changes of selected genes from **(c)** by qRT-PCR ($n = 3$, Mean ± 95% CI, $^{*}p < 0.05$, $^{***}p < 0.001$, one-way ANOVA). Data representative of at least 3 independent experiments.

differentiation effects with DYRK1A knockdown. Furthermore, SRSF4, SRSF5, and SRSF6 knockdowns in hMSCs confirmed the role of this pathway in chondrocyte differentiation, measured by increased *COMP, SOX9,* and *RUNX1* expression, while *RUNX2* and *CTNNB1* were unaffected [Supplementary Fig. 12(a)–(d)].

hMSC differentiation into chondrocytes starts with early chondrocyte condensation followed by differentiation into mature Type II collagen-, aggrecan-, and proteoglycan-producing chondrocytes[31]. CLK2 knockdown induced expression of 30 chondrogenic genes including *ACAN, CD44, COL2A1, DOT1L,* and *COMP,* while DYRK1A knockdown induced upregulation 11 genes (>1.5-fold, $q < 0.05$; Nanostring's nCounter® Vantage 3D™ chondrocyte panel) on day 21 [Fig. 4(g) and (h)]. CLK2+DYRK1A knockdown upregulated 41 genes including *FGFR2, FOXO1, MAPK8, PRG4,* and *TGFβ3* in addition to *ACAN, CD44, COL2A1, DOT1L,* and *COMP,* while TCF7 knockdown upregulated 18 genes. Expression of *CCNG2, CD44, COL2A1, COMP, DOT1L, TGFβ1,* and *TGFβ3* was significantly increased with CLK2+DYRK1A knockdown compared to

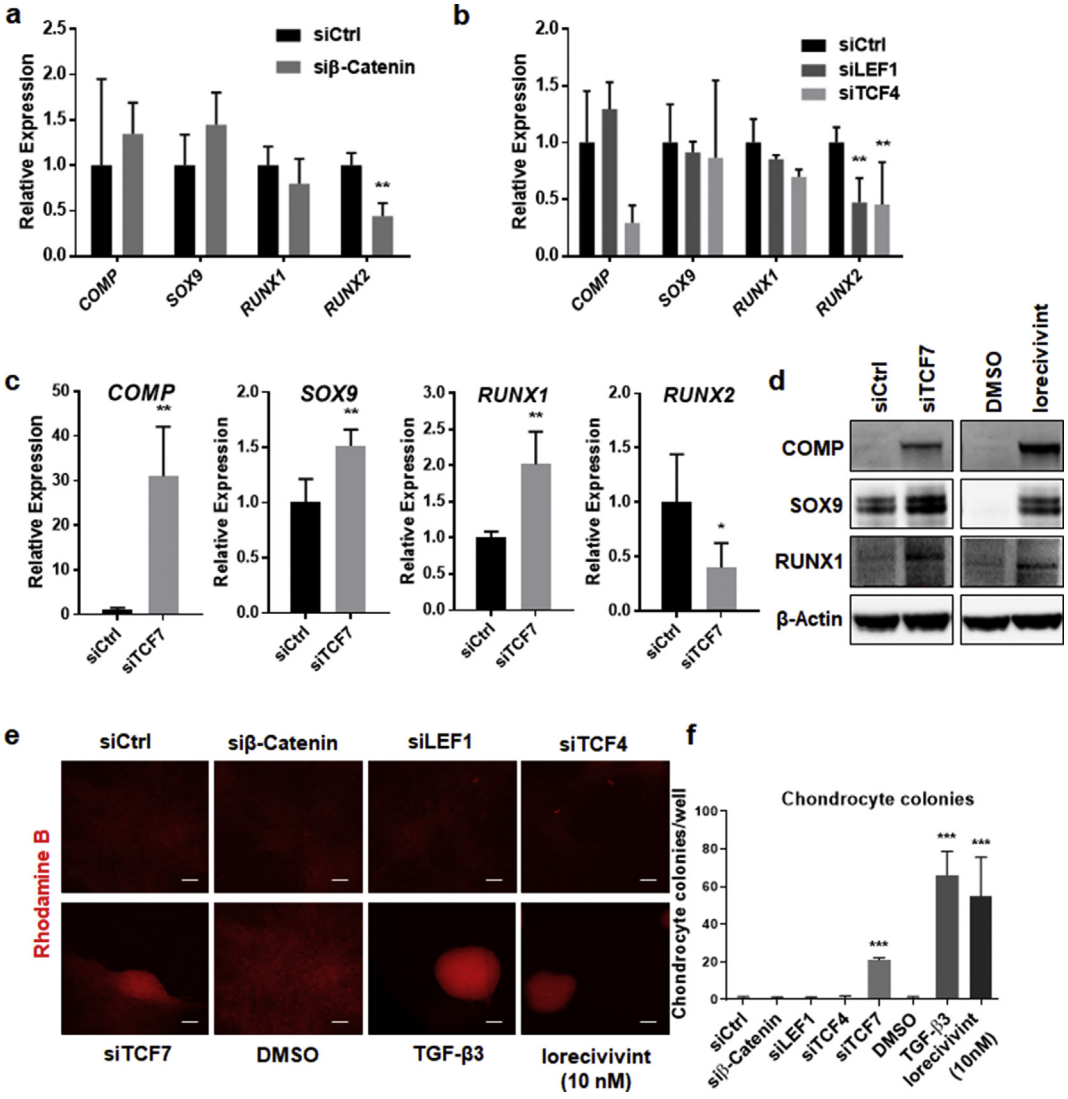

Fig. 3. Inhibition of TCF7 induced early chondrocyte differentiation. **(a–c)** Gene expression of chondrocyte markers *COMP, SOX9,* and *RUNX1* and osteogenic marker *RUNX2* in hMSCs following treatment with either non-targeted control siRNA or siRNA specific to **(a)** β-catenin, **(b)** LEF1 or TCF4, **(c)** TCF7 for 72 hrs, measured by qRT-PCR. Fold change relative to siRNA control ($n = 3$, Mean ± 95% CI, $^{*}p < 0.05$, $^{**}p < 0.01$, *t*-test), and **(d)** Western blot confirmation for **(c)**. β-actin serves as a loading control. **(e)** Representative images of chondrocytes treated with either non-targeted control siRNA or siRNA specific to β-catenin, LEF1, TCF4, TCF7, or DMSO, lorecivivint (10 nM) and stained with Rhodamine B at 10 days. TGF-β3 acts as a positive control for chondrocyte differentiation. Scale bars, 10 μm. **(f)** Quantification of chondrocytes from **(e)** ($n = 3$, Mean ± 95% CI, $^{***}p < 0.001$, one-way ANOVA). Data representative of at least 2 independent experiments.

CLK2 knockdown alone [Fig. 4(g) and (h), Supplementary Fig. 13(a)], indicating a role for DYRK1A inhibition in enhancing the effects of CLK2 inhibition or for maintenance of chondrocyte function.

HIPK2 knockdown had no significant effects on chondrocyte differentiation measured by *COMP, SOX9, RUNX1,* or *RUNX2* expression compared to siCtrl [Supplementary Fig. 12(e)].

Cartilage protection: inhibition of CLK2 and DYRK1A inhibited expression of cartilage catabolic enzymes

The role of CLK2 and DYRK1A in the inhibition of metalloproteinase (MMP) production was evaluated in human chondrocytes using IL-1β- (10 ng/ml) stimulated gene expression of *MMP-1*, *MMP-3*, *MMP-9*, and *MMP-13*. CLK2 knockdown inhibited *MMP-3*, *MMP-9*, and *MMP-13* expression and DYRK1A knockdown inhibited *MMP-9* expression, while CLK2+DYRK1A knockdown inhibited all four proteases [Fig. 4(i), Supplementary Fig. 12(f) and (g)]. Lorecivivint, CC-671, and Harmine inhibited *MMP-1*, *MMP-3*, and *MMP-13* expression, compared to DMSO, with lorecivivint ~100-fold more potent than CC-671 and Harmine [Supplementary Fig. 13(b)].

Anti-inflammatory activity: lorecivivint inhibited inflammatory signaling mediators NF-κB and STAT3

Lorecivivint effects on STAT3, a known target of DYRK1A[32], and other inflammatory mediators in LPS-stimulated THP-1 monocytes were evaluated. Compared to DMSO, lorecivivint (4 hrs) dose dependently decreased phospho-STAT3 (S727, Y705), phospho- and total NF-κB (p105/p50), and phospho-FOXO1/3a, while AKT, JNK1, cJUN, p38/MAPK, and TLR4 were not inhibited. Lorecivivint (20 hrs) robustly inhibited NF-κB, STAT3, JNK1, and FOXO1/3a phosphorylation, while AKT, cJUN, p38/MAPK, and TLR4 remained unchanged [Supplementary Fig. 14(a)]. Lorecivivint inhibited LPS-stimulated gene expression of NF-κB components [*RELA, RELB*;

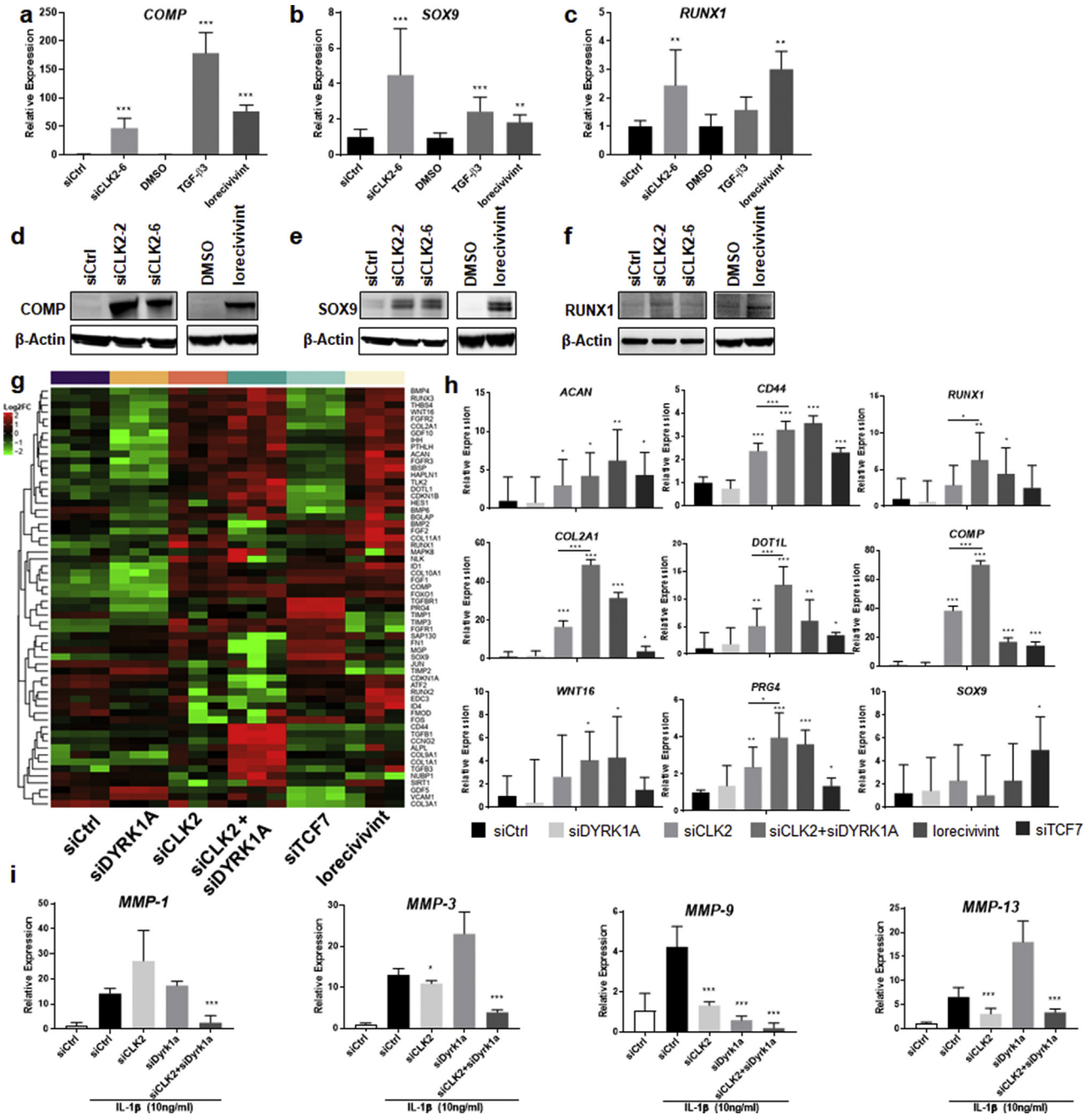

Fig. 4. Inhibition of CLK2 and DYRK1A induced chondrocyte differentiation and protection. **(a–e)** Gene expression of chondrocyte markers **(a, d)** *COMP*, **(b, e)** *SOX9*, and **(c, f)** *RUNX1* in hMSCs at 72 hrs following treatment with either siRNA specific to CLK2 or non-targeted control siRNA, measured by qRT-PCR and Western blot. Lorecivivint and TGF-β3 serve as positive controls for chondrocyte differentiation. Fold change relative to siRNA control ($n = 3$, Mean ± 95% CI, $^{**}p < 0.01$, $^{***}p < 0.001$, one-way ANOVA), β-actin serves as loading control. **(g)** Chondrocyte gene expression in hMSCs at 21 days following treatment with either siRNA specific to CLK2, DYRK1A, CLK2+DYRK1A, TCF7, or non-targeted control siRNA, measured using the Nanostring nCounter® gene array. Lorecivivint serves as a positive control for chondrocyte differentiation. **(h)** Confirmation of gene expression changes of selected genes from **(g)**, by qRT-PCR ($n = 3$, Mean ± 95% CI, $^{*}p < 0.05$, $^{**}p < 0.01$, $^{***}p < 0.001$, one-way ANOVA). **(i)** Gene expression of *MMP-1*, *MMP-3*, *MMP-9*, and *MMP-13* in chondrocytes treated with either siRNA specific to CLK2, DYRK1A, CLK2+DYRK1A, or control siRNA for 72 hrs and then stimulated with IL-1β for 24 hrs, measured by qRT-PCR. Fold change relative to siRNA control ($n = 3$, Mean ± 95% CI, $^{*}p < 0.05$, $^{***}p < 0.001$, one-way ANOVA). Data representative of at least 2 independent experiments.

Supplementary Fig. 14(b)]. Lorecivivint treatment showed no effects on phospho- or total NF-κB (p105/p50) at 10 mins, 30 mins, 1 hr, or 2 hrs but decreased both phospho- and total NF-κB at 4 hrs and 20 hrs, while phospho-STAT3 (Y705) was inhibited at 1 hr, 2 hrs, 4 hrs, and 20 hrs with no effects on total STAT3 at any time point (Supplementary Fig. 15). Lorecivivint inhibited the expression of NF-κB pathway genes (*NFKB1*, *NFKB2*, *RELA*, *RELB*, and *BCL3*) without effects on NF-κB inhibitors (*NFKBIA*, *NFKBIB*, *IKKβ*, and *IKKγ*; Supplementary Fig. 16). Lorecivivint inhibition of NF-κB and STAT3 were confirmed in synovial fibroblasts and PBMCs [Fig. 5(a)

and (b)]. Lorecivivint was more potent than Harmine or CC-671 in the inhibition of NF-κB and STAT3 in LPS-stimulated PBMCs [Supplementary Fig. 17(a)].

Anti-inflammation: lorecivivint demonstrated potent anti-inflammatory effects in vitro

Lorecivivint dose dependently inhibited IL-6 and TNF-α production in IL-1β- and LPS-stimulated synovial fibroblasts [Fig. 5(c) and (d)] and LPS-stimulated THP-1 cells with EC_{50} = 25–35nM [Supplementary Fig. 17(b)]. Lorecivivint inhibited a panel of inflammatory cytokines in LPS-stimulated synovial fibroblasts [Fig. 5(e)] and LPS- or super antigen-stimulated PBMCs [Fig. 5(f), Supplementary Fig. 17(c)]. Lorecivivint anti-inflammatory activity (decreased IL-6 production) in LPS-stimulated THP-1 cells was comparable to benchmark immune suppressants dexamethasone, cyclosporin A, and prednisolone[33,34] [Supplementary Fig. 17(d)].

Anti-inflammation: inhibition of DYRK1A and CLK2 together reduced inflammatory cytokine production

In THP-1 cells and synovial fibroblasts, CLKs 1-3 and DYRK1A localized in the nucleus, while CLK4 was predominantly in the cytoplasm [Supplementary Fig. 18(a)]. In synovial fibroblasts and PBMCs, lorecivivint dose dependently inhibited SRSF phosphorylation [Fig. 5(g) and (h)] and was more potent than CC-671, while Harmine had no effects [Supplementary Fig. 18(b) and (c)]. Commercial CLK2 or DYRK1A inhibitors demonstrated 100–1,200-fold less potent anti-inflammatory activity than lorecivivint [Supplementary Fig. 18(d)]. Lorecivivint, CC-671, and Harmine also inhibited CHIR99021-stimulated *AXIN2, TCF4, TCF7,* and *LEF1* expression in synovial fibroblasts [Supplementary Fig. 18(e)].

Technical limitations to siRNA-mediated knockdowns led to <80% knockdowns in THP-1 cells, PBMCs, and synovial fibroblasts (data not shown). BEAS-2B, bronchial epithelial cells, respond to LPS stimulation and produce proinflammatory cytokines[35]. Lorecivivint dose dependently inhibited IL-1β- or LPS-stimulated expression and secretion of IL-1β, IL-6, and TNF-α [Supplementary Fig. 19(a)]. In BEAS-2B cells, CLKs 1-3 and DYRK1A were expressed and localized similarly to synovial fibroblasts [Supplementary Fig. 19(b)]. Lorecivivint inhibited phospho-SRSF, phospho- and total NF-κB, and phospho-STAT3 and CHIR99021-stimulated *AXIN2, LEF1, TCF4,* and *TCF7* expression and was more potent than CC-671 and Harmine [Supplementary Fig. 19(c)–(e)].

siRNA knockdowns [Supplementary Fig. 20(a) and (b)] followed by LPS stimulation resulted in decreased *IL-6*, *TNF-α,* and *IL-1β* expression with DYRK1A knockdown and decreased levels of *TNF-α*, *IL-8,* and *IL-1β* with CLK2 knockdown compared to siCtrl. Combined CLK2 and DYRK1A knockdown significantly decreased *IL-6*, *IL-8*, *TNF-α,* and *IL-1β* gene expression and IL-6 and IL-8 protein compared to siCtrl or CLK2 knockdown [Fig. 6(a) and (b)]. CLK3 knockdown had no significant effects on cytokine production [Supplementary Fig. 20(c)].

HIPK2 knockdown showed small decreases in IL-6 and IL-1β expression with no effects on TNF-α and IL-8 expression in LPS-stimulated BEAS-2B cells [Supplementary Fig. 20(d)–(f)]. Since lorecivivint inhibited NF-κB and STAT3, knockdowns of RelA, RelB, and STAT3 were shown to decrease LPS-stimulated IL-6 expression [Supplementary Fig. 21(a)–(d)]. Furthermore, TCF7 knockdown decreased *IL-6*, *TNF-α*, *IL-8,* and *IL-1β* expression compared to siCtrl [Supplementary Fig. 21(e) and (f)].

Anti-inflammation and cartilage protection in vivo: lorecivivint inhibited inflammation, protected cartilage, and improved pain and function in the monosodium iodoacetate (MIA)-induced rat knee OA model

IA MIA causes local inflammation, cartilage degeneration, and increased pain in the joint[36,37]. Lorecivivint [0.3 μg, single IA injection; Supplementary Fig. 22(a)] in MIA-injected rats decreased inflammatory cytokine gene expression (TNF-α, IL-6, IL-8) and protein levels (IL-1β, IL-4, IL-6, IL-8, TNF-α, CXCL10) and catabolic enzymes (MMP-1, MMP-13, ADAMTS5) in the cartilage compared to vehicle [Fig. 7(a) and (b), Supplementary Fig. 22(b)]. Histological examination of the joints 11 days post MIA injection showed inflammatory cells in the synovial membrane and significant increase in the synovial membrane thickness in vehicle-treated rats. In contrast, lorecivivint treatment decreased inflammatory cell infiltrates, synovial membrane thickness, and cytokines (IL-1β, IL-6, TNF-α) compared to vehicle [Fig. 7(c) and (d), Supplementary Fig. 23]. On day 28, Safranin O-Fast Green staining showed loss of smooth cartilage articular surface in vehicle-treated rats, while lorecivivint treatment showed modest increases in articular cartilage and smooth cartilage surface [Fig. 7(e)]. Lorecivivint treatment significantly decreased the histomorphometrical modified OARSI score[38] compared to vehicle [Fig. 7(f)]. Additionally, lorecivivint decreased pain (paw withdrawal threshold measured by Von Frey apparatus) and improved the weight distribution on the injected limb (gait measured by incapacitance meter) compared to vehicle. Beneficial effects on both pain and function with a single IA injection of lorecivivint were sustained through study completion [Fig. 7(g) and (h)].

Lorecivivint inhibited CLK2 and DYRK1A and Wnt signaling in vivo

In vivo pharmacodynamic effects of lorecivivint in cartilage were evaluated in the ACLT+pMMx and MIA models of OA. Lorecivivint (single IA injection- 0.1 μg, 0.3 μg, 1 μg), one week post ACLT+pMMx, decreased phospho-SRSF, SRSF1, AXIN2, TCF7, phospho-SIRT1, phospho-FOXO1, and phospho-STAT3 compared to vehicle at day 35 [Fig. 8(a)]. Lorecivivint decreased CLK2, DYRK1A, SRSF1, SRSF5, and SRSF6 expression compared to vehicle [Fig. 8(b)]. Furthermore, lorecivivint decreased expression of 19 genes and increased expression of 8 genes [Nanostring Wnt panel, Fig. 8(c)], confirmed by qPCR for AXIN2, TCF7, DVL1, TCF4, CTGF, and BTRC [Fig. 8(d)]. In the MIA model, 4 days after single IA injection, lorecivivint decreased phosphorylation of SRSF, NF-κB, STAT3, and FOXO1 compared to vehicle [Fig. 8(e)]. While no changes in the total protein levels of SRSF1 and STAT3 were observed, lorecivivint decreased protein levels of total NF-κB and increased protein levels of total FOXO1 [Fig. 8(a), (e)].

Discussion

Lorecivivint is a first-in-class, reversible, ATP-competitive, small-molecule Wnt pathway inhibitor with selectivity towards kinases primarily from the CMGC kinase group. Through biochemical and genetic studies, the intranuclear kinases CLK2 and DYRK1A were demonstrated to be critical in the phenotypic activity of lorecivivint. These kinases were also validated, for the first time, as novel targets for Wnt pathway modulation, which is associated with chondrocyte differentiation, inhibition of cartilage degradation, and anti-inflammation.

The Wnt pathway is subject to complex regulation, including at the posttranscriptional level[39–42]. Previous strategies targeting the canonical Wnt pathway, including targeting β-catenin or Wnt pathway molecules upstream of β-catenin, have not resulted in

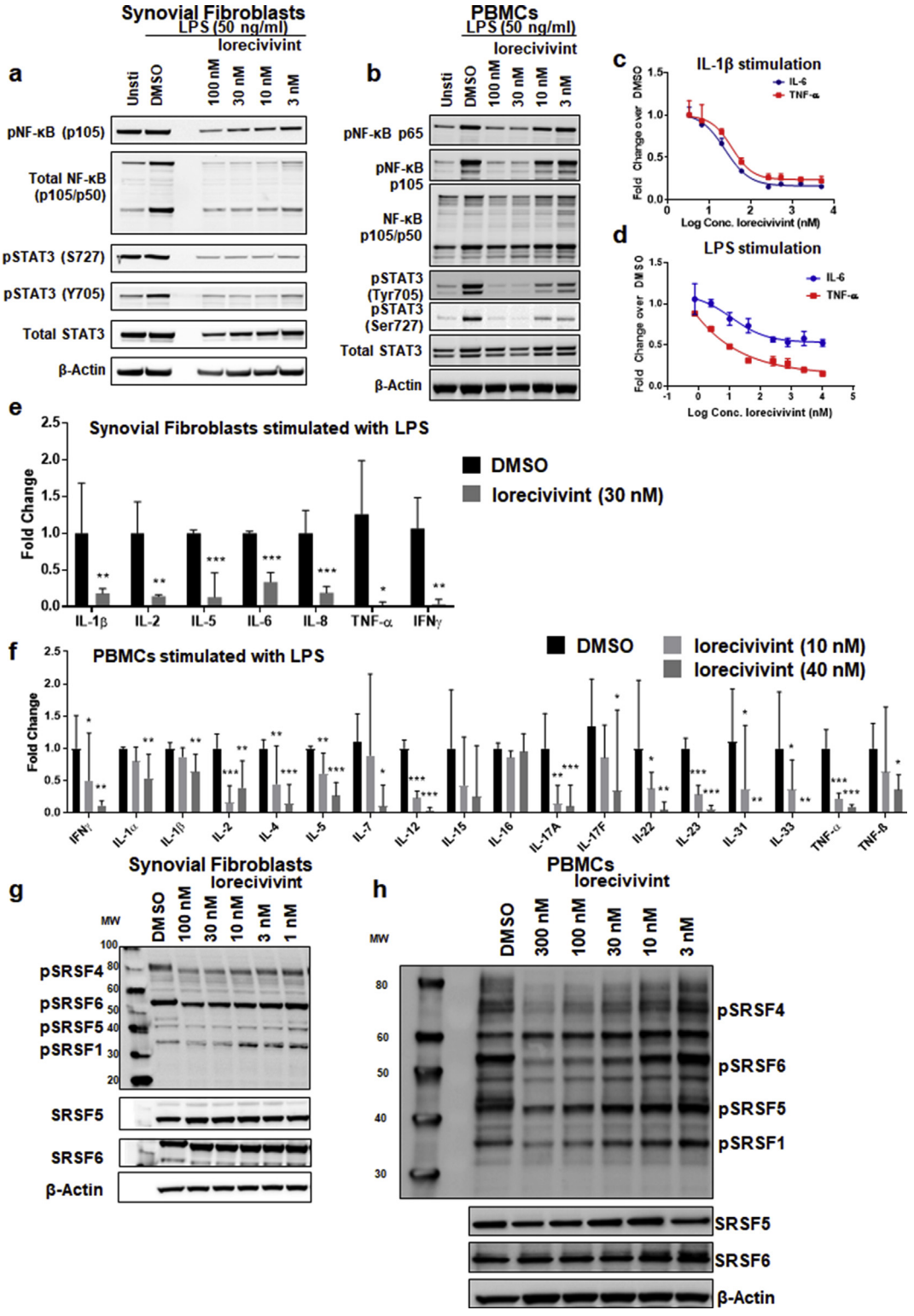

Fig. 5. Lorecivivint inhibited inflammatory responses in synovial fibroblasts and PBMCs. **(a, b)** Expression of phospho- and total NF-κB and STAT3 in **(a)** synovial fibroblasts and **(b)** PBMCs stimulated with LPS and treated with DMSO or lorecivivint for 20 hrs, measured by Western blot. β-actin serves as a loading control. **(c, d)** Inhibition of IL-6 and TNF-α production in synovial fibroblasts stimulated with **(c)** IL-1β or **(d)** LPS and treated with DMSO or lorecivivint for 24 hrs, measured by HTRF and ELISA ($n = 3$, Mean ± SEM). **(e, f)** Production of pro-inflammatory cytokines in **(e)** synovial fibroblasts and **(f)** PBMCs stimulated with LPS and treated with DMSO or lorecivivint for 72 hrs, measured by MSD-based ELISA ($n = 3$, Mean ± 95% CI, $^{*}p < 0.05$, $^{**}p < 0.01$, $^{***}p < 0.001$, *t*-test, one-way ANOVA). **(g, h)** Western blot of phospho- and total SRSF in **(g)** synovial fibroblasts and **(h)** PBMCs following treatment with lorecivivint or DMSO for 1 hr. β-actin serves as a loading control. Data representative of at least 2 independent experiments.

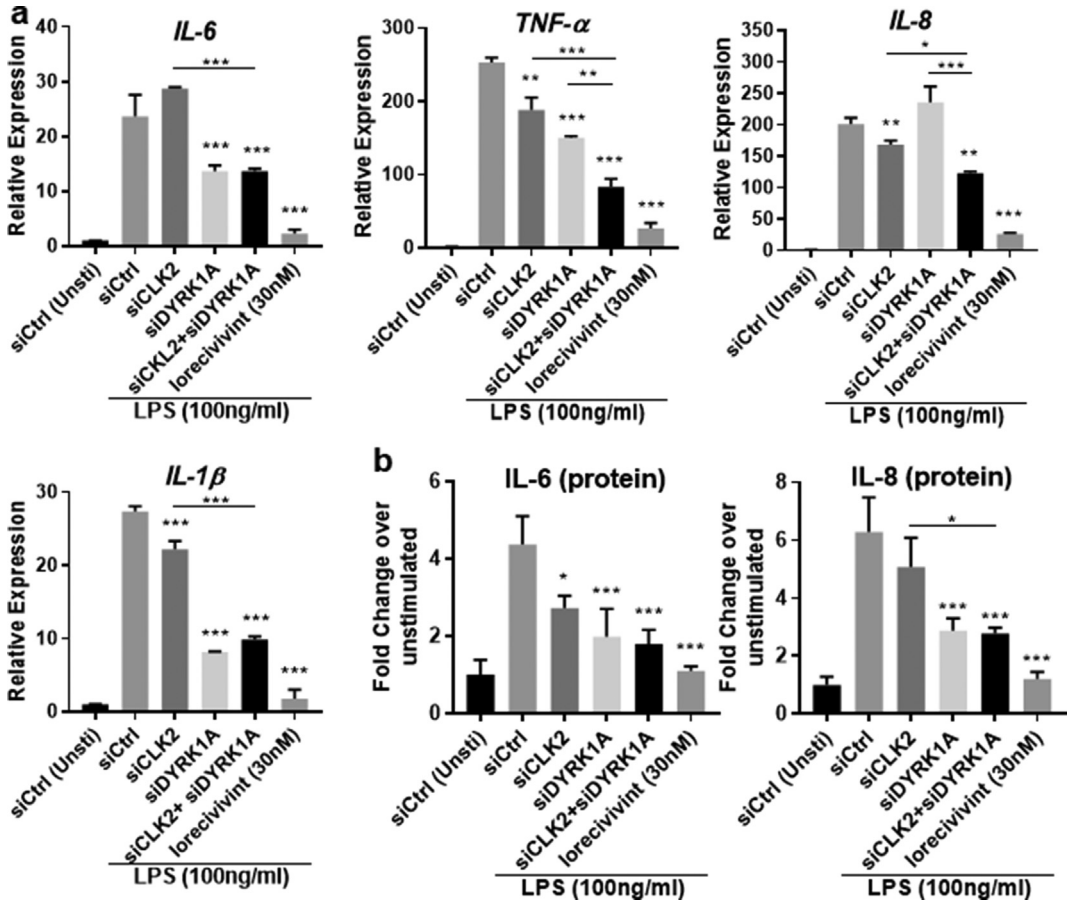

Fig. 6. Inhibition of DYRK1A and CLK2 together reduced inflammatory cytokine production. **(a, b)** Gene expression of **(a)** *IL-6*, *TNF-α*, *IL-8*, and *IL-1β* in BEAS-2B cells treated with siRNA specific to CLK2, DYRK1A, CLK2+DYRK1A, or lorecivivint or non-targeted control siRNA and stimulated with LPS for 6 hrs, measured by qRT-PCR. Fold change relative to unstimulated siRNA control ($n = 3$, Mean ± 95% CI, $^{*}p < 0.05$, $^{**}p < 0.01$, $^{***}p < 0.001$, one-way ANOVA). **(b)** IL-6 and IL-8 protein production in BEAS-2B cells treated with siRNA specific to CLK2, DYRK1A, CLK2+DYRK1A, or lorecivivint or non-targeted control siRNA and stimulated with LPS for 6 hrs, measured by HTRF-based assay ($n = 3$, Mean ± 95% CI, $^{*}p < 0.05$, $^{***}p < 0.001$, one-way ANOVA). Data representative of at least 3 independent experiments.

FDA-approved drugs[43,44] due to off-target or non-selective pharmacodynamic effects. There were no previously reported compounds which modulated Wnt pathway activity downstream or independent of β-catenin. Knockdown of β-catenin in hMSCs inhibited Wnt signaling but did not induce chondrocyte differentiation *in vitro*, indicating that more selective regulation of Wnt target genes downstream of β-catenin or β-catenin-sparing mechanisms of Wnt pathway modulation may be necessary for chondrogenesis. Lorecivivint treatment and CLK2 and DYRK1A knockdowns demonstrated decreased expression of Wnt target genes independent of β-catenin while upregulating secreted Wnt pathway inhibitors in hMSCs, chondrocytes, and BEAS2B cells. These data, along with observations that lorecivivint inhibited the expression of genes not directly regulated by β-catenin, Wnt pathway receptors, or ligands suggested that lorecivivint, through its effects on CLK2 and DYRK1A, regulated these Wnt pathway genes via a β-catenin-independent mechanism.

Chondrocyte differentiation and function have previously been shown to be under tight control by the Wnt pathway[45,46]. A novel role of CLK2 inhibition in chondrocyte differentiation from hMSCs and DYRK1A inhibition in enhancing chondrocyte function was demonstrated by the upregulation of several early and late chondrogenic markers in cells treated with CLK2 and DYRK1A siRNAs. Downregulation of *TCF7* by lorecivivint as well as CLK2 and DYRK1A knockdowns was shown to be essential and sufficient for induction of chondrocyte differentiation. Data demonstrating chondrogenesis with TCF7 knockdown but not with β-catenin, LEF1, and TCF4 knockdown further supports the notion that chondrogenesis involves complex modulation of the Wnt signaling pathway rather than general inhibition. Lorecivivint, by acting downstream and independent of β-catenin in hMSCs, could provide specific regulation of the components involved in chondrocyte differentiation and function.

Inhibition of the Wnt pathway activity with CLK2 knockdown and CLK2-specific inhibitors supported involvement of CLK2 or its downstream components in regulating Wnt signaling at a posttranscriptional level, possibly through alternative splicing of Wnt target genes. The loss or inhibition of CLK2 may have impacted pre-mRNA processing of genes (e.g., *TCF7*), leading to formation of unstable transcripts and overall inhibitory effects on subsequent gene expression[47,48]. While the effects of lorecivivint appear to be mediated through alternative splicing of Wnt pathway genes, alternative splicing of other genes cannot be ruled out. DYRK1A inhibition by lorecivivint inhibited SIRT1, a positive regulator of the Wnt pathway[49,50], and promoted activation of FOXO1, resulting in inhibition of Wnt pathway gene expression, promoting cartilage protection, and enhancing chondrocyte function *in vitro* and *in vivo*. By targeting both CLK2 and DYRK1A, lorecivivint provided favorable effects on both chondrocyte differentiation and function compared to targeting the kinases individually.

Inhibition of cartilage degradation has the potential to modify OA progression. Lorecivivint previously demonstrated inhibition of

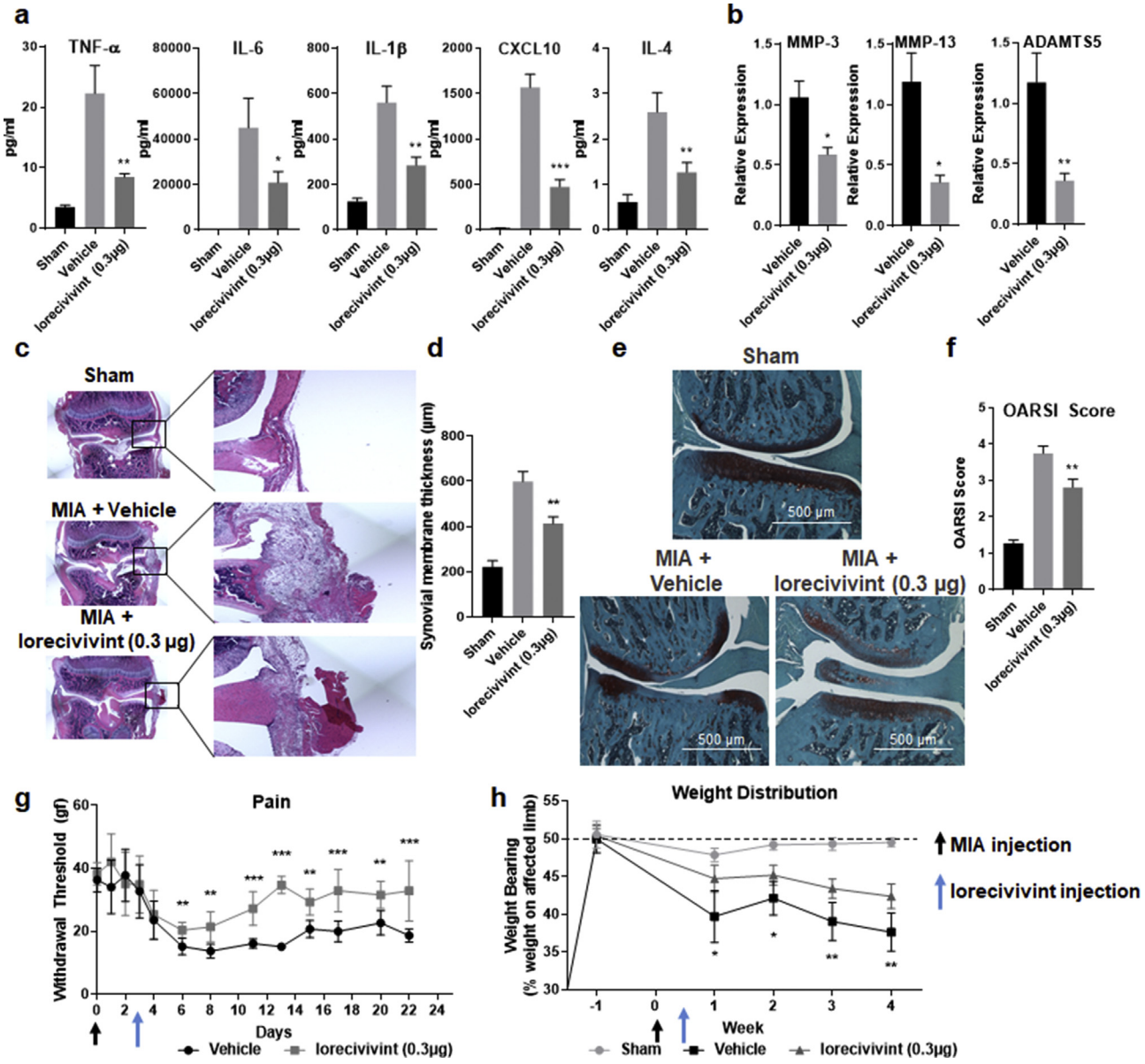

Fig. 7. Lorecivivint inhibited inflammation, protected cartilage, and improved pain and function in the monosodium iodoacetate (MIA)-induced rat knee OA model. MIA-injected rats treated with IA injection of either vehicle or lorecivivint (0.3 μg) and cartilage isolated at day 4, 11, 28. **(a)** Production of TNF-α, IL-6, IL-1β, CXCL10, and IL-4 in the cartilage of rats on day 4, measured using an MSD-based ELISA assay ($n = 8$, Mean ± 95% CI, $^{*}p < 0.05$, $^{**}p < 0.01$, $^{***}p < 0.001$, one-way ANOVA). **(b)** Gene expression of MMP-3, MMP-13, and ADAMTS5 in the cartilage of rats on day 4, measured by qRT-PCR ($n = 8$, Mean ± 95% CI, $^{*}p < 0.05$, $^{**}p < 0.01$, one-way ANOVA). **(c)** Representative images of the knee joint stained with H&E from sham-, vehicle-, or lorecivivint-treated rats on day 11. **(d)** Quantification of the synovial membrane thickness, measured from images in **(c)** ($n = 10$ rats, Mean ± 95% CI, $^{**}p = 0.0014$, one-way ANOVA). **(e)** Representative images of medial tibial plateau of the knee joint stained with Safranin O-Fast Green from sham-, vehicle-, or lorecivivint-treated rats on day 28 (scale bars, 500 μm). (**f**) The medial tibial plateau joint score based on the OARSI scoring system ($n = 10$ rats, Mean ± 95% CI, $^{**}p = 0.0022$, one-way ANOVA). **(g)** Pain measurements using the Von Frey apparatus in rats injected with MIA and treated with either vehicle or lorecivivint represented as paw withdrawal threshold (gram-force) ($n = 10$ rats, Mean ± 95% CI, $^{**}p < 0.01$, $^{***}p < 0.001$, baseline-adjusted, repeated measures ANOVA). **(h)** Weight distribution on the hind limbs using the Incapacitance meter in rats injected with MIA and treated with either vehicle or lorecivivint ($n = 10$ rats, Mean ± 95% CI, $^{*}p < 0.05$, $^{**}p < 0.01$, baseline-adjusted, repeated measures ANOVA). Data representative of at least 2 independent experiments.

cartilage catabolic enzymes *in vitro* and *in vivo* under pathophysiological OA-like conditions[14]. Inhibition of CLK2 and DYRK1A each inhibited IL-1β-induced MMP expression, providing mechanisms for lorecivivint's chondroprotective properties. Lorecivivint also reduced protease expression in articular cartilage in the inflammatory MIA model compared to vehicle.

In addition to its beneficial effects on cartilage, lorecivivint exhibited potent and broad anti-inflammatory profile *in vitro* and *in vivo*. Pharmacological and genetic DYRK1A inhibition, through its effects on STAT3, was shown to be sufficient for inhibition of inflammatory cytokine production. Knockdown of CLK2 further enhanced the effects of DYRK1A knockdown, possibly through its effects on NF-κB. DYRK1A and CLK2 are novel targets for anti-inflammatory activity with independent and potentially synergistic anti-inflammatory effects. In the inflammatory MIA model of OA, a single IA injection of lorecivivint reduced inflammation and cartilage catabolism with subsequently decreased pain and improved weight-bearing function compared to vehicle.

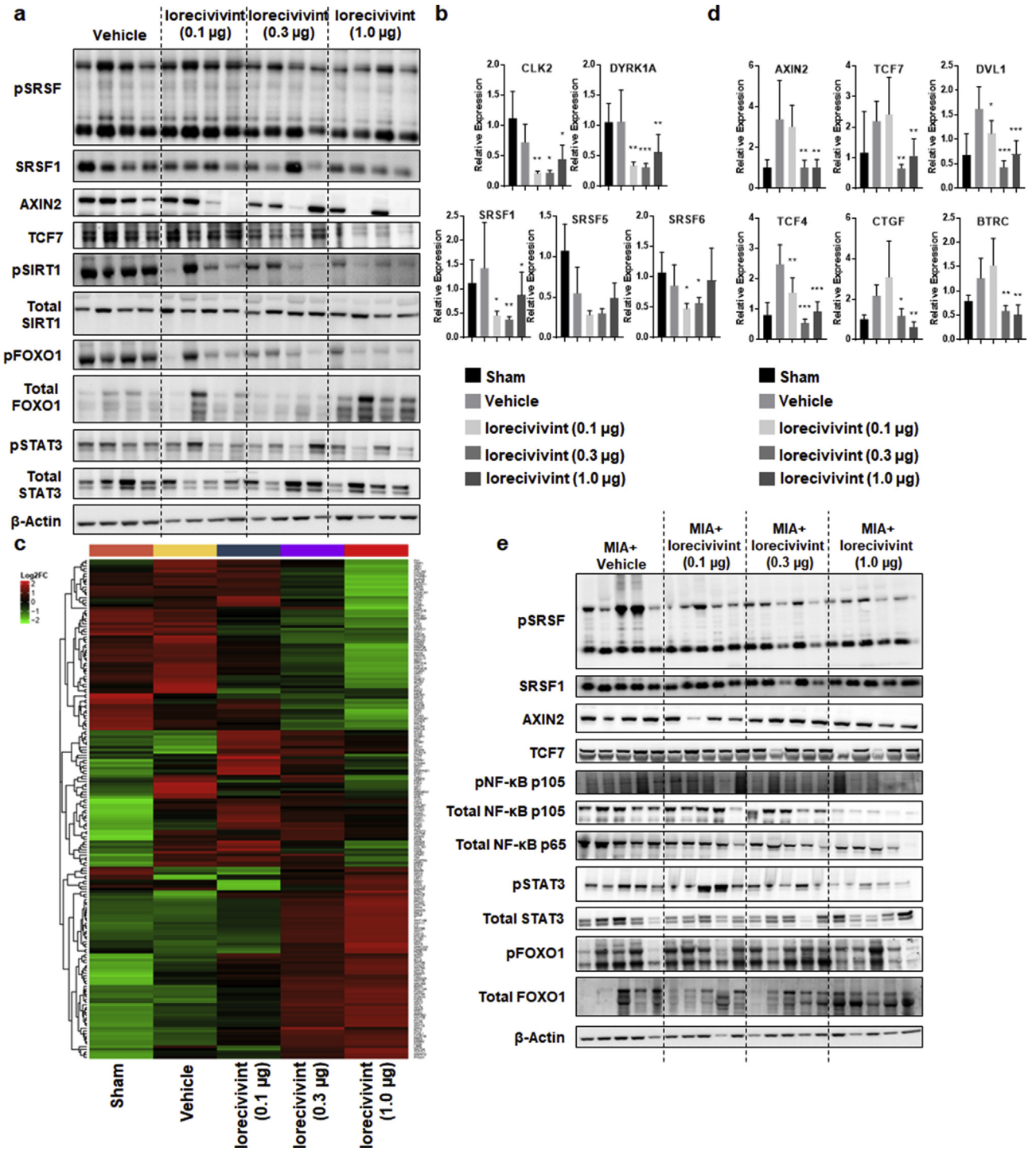

Fig. 8. Lorecivivint inhibited the Wnt pathway, CLK2, and DYRK1A signaling *in vivo* in the ACLT+pMMx model and the MIA model of rat knee OA. ACLT+pMMx rats treated with IA injection of either vehicle or lorecivivint (0.1 μg, 0.3 μg, 1.0 μg) 1 week after surgery and cartilage isolated at day 35 **(a)** Western blots for phospho-SRSF, SRSF1, AXIN2, TCF7, phospho-SIRT1, total SIRT1, phospho-FOXO1, total FOXO1, phospho-STAT3, and total STAT3 in the cartilage. β-actin serves as a loading control. **(b)** Gene expression of CLK2, DYRK1A, SRSF1, SRSF5, and SRSF6 in cartilage, measured by qRT-PCR ($n = 8$, Mean ± 95% CI, $^{*}p < 0.05$, $^{**}p < 0.01$, $^{***}p < 0.001$, one-way ANOVA). **(c)** Wnt pathway gene expression in cartilage, measured using the Nanostring nCounter® gene array. **(d)** Confirmation of gene expression changes of selected genes from **(c)** by qRT-PCR ($n = 8$, Mean ± 95% CI, $^{*}p < 0.05$, $^{**}p < 0.01$, $^{***}p < 0.001$, one-way ANOVA). **(e)** MIA-injected rats treated with IA injection of either vehicle or lorecivivint (0.1 μg, 0.3 μg, 1.0 μg) and cartilage isolated at day 11. Western blots for phospho-SRSF, SRSF1, AXIN2, TCF7, phospho-NF-κB, total NF-κB, phospho-STAT3, total STAT3, phospho-FOXO1, and total FOXO1 in the cartilage. β-actin serves as a loading control. Data representative of at least 2 independent experiments.

There is a tremendous unmet need for improved OA therapeutic agents. Current treatments only focus on pain or inflammation and most agents in development only target one aspect of the disease. While previously reported compounds targeting CLKs or DYRK1A lack either the kinase specificity or the cellular potency to be potential therapeutic candidates, lorecivivint demonstrated modulation of the Wnt pathway, chondrogenesis, cartilage protection, and anti-inflammatory properties. While CLK2 and DYRK1A appear to

be the primary targets of lorecivivint for Wnt pathway inhibition, chondrocyte differentiation, and protection, in addition to anti-inflammation, contributions from CLK1, CLK3, CLK4 and other cellular proteins or pathways cannot be ruled out. *In vivo* studies suggested lorecivivint remains local after IA injection, and the effects observed in preclinical models support its therapeutic potential. In human clinical trials (NCT02095548, NCT02536833, NCT03122860), lorecivivint appeared to be safe and well tolerated, and these studies support lorecivivint as a potential symptom- and structure-modifying treatment for knee OA. Future work will reveal additional insights into regulation of gene expression and cellular phenotypes by lorecivivint, CLK2, DYRK1A and their interactions.

Through the elucidation of lorecivivint's mechanism of action, we have revealed previously unreported regulatory links between CLK2, DRYK1A, and the Wnt pathway as well as chondrogenesis and inflammation [Supplementary Fig. 22(c)]. Lorecivivint, through a dual-target mechanism, shows potential as a single agent to provide both symptom relief and disease modification through its anti-inflammatory and cartilage-beneficial effects.

Author contributions

Conception and design: Vishal Deshmukh, Alyssa Lauren O'Green, Carine Bossard, Tim Seo, Sunil KC, Charlene Barroga, Yusuf Yazici.

Acquisition, analysis and interpretation of data: Vishal Deshmukh, Alyssa Lauren O'Green, Carine Bossard, Tim Seo, Lisa Lamangan, Maureen Ibanez, Abdullah Ghias, Carolyn Lai, Long Do, Shawn Cho, Joseph Cahiwat, Kevin Chiu, Melinda Pedraza, Scott Anderson, Rodney Harris, Luis Dellamary, Sunil KC, Charlene Barroga, Benoit Melchior, Sarah Kennedy, Jeymi Tambiah, Betty Tam, Yusuf Yazici.

Drafting the article: Vishal Deshmukh, Alyssa Lauren O'Green, Sarah Kennedy, Jeymi Tambiah, Yusuf Yazici.

Final approval of the article: Vishal Deshmukh, Alyssa Lauren O'Green, Carine Bossard, Tim Seo, Lisa Lamangan, Maureen Ibanez, Abdullah Ghias, Carolyn Lai, Long Do, Shawn Cho, Joseph Cahiwat, Kevin Chiu, Melinda Pedraza, Scott Anderson, Rodney Harris, Luis Dellamary, Sunil KC, Charlene Barroga, Benoit Melchior, Sarah Kennedy, Jeymi Tambiah, Betty Tam, John Hood, Yusuf Yazici.

Conflict of Interest

Samumed LLC salary and equity: Vishal Deshmukh, Alyssa Lauren O'Green, Carine Bossard, Tim Seo, Lisa Lamangan, Maureen Ibanez, Abdullah Ghias, Carolyn Lai, Long Do, Shawn Cho, Joseph Cahiwat, Kevin Chiu, Melinda Pedraza, Scott Anderson, Rodney Harris, Luis Dellamary, Sunil KC, Charlene Barroga, Benoit Melchior, Sarah Kennedy, Jeymi Tambiah, Yusuf Yazici.

Samumed LLC equity: John Hood, Betty Tam.

Financial support

Financial support for this study and its publication was provided by Samumed, LLC.

Acknowledgements

We thank Christopher Swearingen, PhD for assistance with statistical analysis, Mirta Grifman, PhD and Hutch Humphreys, M.S. for discussions and critical revision of the manuscript, and Selin Esener, M.S. and Elizabeth Orient, M.A. for assistance with copy-editing and artwork.

Supplementary data

Supplementary data to this article can be found online at https://doi.org/10.1016/j.joca.2019.05.006.

References

1. Lawrence RC, Felson DT, Helmick CG, Arnold LM, Choi H, Deyo RA, *et al.* Estimates of the prevalence of arthritis and other rheumatic conditions in the United States. Part II. Arthritis Rheum 2008;58:26–35.
2. Howell DS. Pathogenesis of osteoarthritis. Am J Med 1986;80:24–8.
3. Johnson K, Zhu S, Tremblay MS, Payette JN, Wang J, Bouchez LC, *et al.* A stem cell-based approach to cartilage repair. Science 2012;336:717–21.
4. Gigout A, Guehring H, Froemel D, Meurer A, Ladel C, Reker D, *et al.* Sprifermin (rhFGF18) enables proliferation of chondrocytes producing a hyaline cartilage matrix. Osteoarthritis Cartilage 2017;25:1858–67.
5. Li N-G, Shi Z-H, Tang Y-P, Wang Z-J, Song S-L, Qian L-H, *et al.* New hope for the treatment of osteoarthritis through selective inhibition of MMP-13. Curr Med Chem 2011;18:977–1001.
6. Nakata K, Hanai T, Take Y, Osada T, Tsuchiya T, Shima D, *et al.* Disease-modifying effects of COX-2 selective inhibitors and non-selective NSAIDs in osteoarthritis: a systematic review. Osteoarthritis Cartilage 2018;26:1263–73.
7. Clevers H. Wnt/beta-Catenin signaling in development and disease. Cell 2006;127:469–80.
8. Clevers H, Loh KM, Nusse R. Stem cell signaling. An integral program for tissue renewal and regeneration: Wnt signaling and stem cell control. Science 2014;346:1248012.
9. Zhu M, Chen M, Zuscik M, Wu Q, Wang YJ, Rosier RN, *et al.* Inhibition of β-catenin signaling in articular chondrocytes results in articular cartilage destruction. Arthritis Rheum 2008;58:2053–64.
10. Zhu M, Tang D, Wu Q, Hao S, Chen M, Xie C, *et al.* Activation of β-catenin signaling in articular chondrocytes leads to osteoarthritis-like phenotype in adult β-catenin conditional activation mice. J Bone Miner Res 2009;24:12–21.
11. Luyten FP, Tylzanowski P, Lories RJ. Wnt signaling and osteoarthritis. Bone 2009;44:522–7.
12. Levine M, Tjian R. Transcription regulation and animal diversity. Nature 2003;424:147–51.
13. Smith CW, Valcárcel J. Alternative pre-mRNA splicing: the logic of combinatorial control. Trends Biochem Sci 2000;25:381–8.
14. Deshmukh V, Hu H, Barroga C, Bossard C, KC S, Dellamary L, *et al.* A small-molecule inhibitor of the Wnt pathway (SM04690) as a potential disease modifying agent for the treatment of osteoarthritis of the knee. Osteoarthritis Cartilage 2017;26:18–27.
15. Rosenthal AS, Tanega C, Shen M, Mott BT, Bougie JM, Nguyen D-T, *et al.* An Inhibitor of the Cdc2-like Kinase 4 (Clk4). Probe Reports from the NIH Molecular Libraries Program 2010.
16. Coombs TC, Tanega C, Shen M, Wang JL, Auld DS, Gerritz SW, *et al.* Small-molecule pyrimidine inhibitors of the cdc2-like (Clk) and dual specificity tyrosine phosphorylation-regulated (Dyrk) kinases: development of chemical probe ML315. Bioorg Med Chem Lett 2013;23:3654–61.
17. Naert G, Ferré V, Meunier J, Keller E, Malmström S, Givalois L, *et al.* Leucettine L41, a DYRK1A-preferential DYRKs/CLKs inhibitor, prevents memory impairments and neurotoxicity induced by oligomeric Aβ25-35 peptide administration in mice. Eur Neuropsychopharmacol 2015;25:2170–82.
18. Muraki M, Ohkawara B, Hosoya T, Onogi H, Koizumi J, Koizumi T, *et al.* Manipulation of alternative splicing by a newly developed inhibitor of Clks. J Biol Chem 2004;279:24246–54.
19. Riggs JR, Nagy M, Elsner J, Erdman P, Cashion D, Robinson D, *et al.* The discovery of a dual TTK protein kinase/CDC2-like

kinase (CLK2) inhibitor for the treatment of triple negative breast cancer initiated from a phenotypic screen. J Med Chem 2017;60:8989–9002.
20. Ogawa Y, Nonaka Y, Goto T, Ohnishi E, Hiramatsu T, Kii I, *et al*. Development of a novel selective inhibitor of the Down syndrome-related kinase Dyrk1A. Nat Commun 2010;1:86.
21. Monteiro MB, Ramm S, Chandrasekaran V, Boswell SA, Weber EJ, Lidberg KA, *et al*. A high-throughput screen identifies DYRK1A inhibitor ID-8 that stimulates human kidney tubular epithelial cell proliferation. J Am Soc Nephrol 2018, https://doi.org/10.1681/ASN.2018040392.
22. De la Torre R, De Sola S, Pons M, Duchon A, de Lagran MM, Farré M, *et al*. Epigallocatechin-3-gallate, a DYRK1A inhibitor, rescues cognitive deficits in Down syndrome mouse models and in humans. Mol Nutr Food Res 2014;58:278–88.
23. Göckler N, Jofre G, Papadopoulos C, Soppa U, Tejedor FJ, Becker W. Harmine specifically inhibits protein kinase DYRK1A and interferes with neurite formation. FEBS J 2009;276:6324–37.
24. Duncan PI, Stojdl DF, Marius RM, Scheit KH, Bell JC. The Clk2 and Clk3 dual-specificity protein kinases regulate the intranuclear distribution of SR proteins and influence pre-mRNA splicing. Exp Cell Res 1998;241:300–8.
25. Colwill K, Pawson T, Andrews B, Prasad J, Manley JL, Bell JC, *et al*. The Clk/Sty protein kinase phosphorylates SR splicing factors and regulates their intranuclear distribution. EMBO J 1996;15:265–75.
26. Guo X, Williams JG, Schug TT, Li X. DYRK1A and DYRK3 promote cell survival through phosphorylation and activation of SIRT1. J Biol Chem 2010;285:13223–32.
27. Woods YL, Rena G, Morrice N, Barthel A, Becker W, Guo S, *et al*. The kinase DYRK1A phosphorylates the transcription factor FKHR at Ser329 in vitro, a novel in vivo phosphorylation site. Biochem J 2001;355:597–607.
28. Akasaki Y, Hasegawa A, Saito M, Asahara H, Iwamoto Y, Lotz MK. Dysregulated FOXO transcription factors in articular cartilage in aging and osteoarthritis. Osteoarthritis Cartilage 2014;22:162–70.
29. Matsuzaki T, Alvarez-Garcia O, Mokuda S, Nagira K, Olmer M, Gamini R, *et al*. FoxO transcription factors modulate autophagy and proteoglycan 4 in cartilage homeostasis and osteoarthritis. Sci Transl Med 2018;10.
30. Kim EA, Kim JE, Sung KS, Choi DW, Lee BJ, Choi CY. Homeodomain-interacting protein kinase 2 (HIPK2) targets β-catenin for phosphorylation and proteasomal degradation. Biochem Biophys Res Commun 2010;394:966–71.
31. Dahlin R, Ni M, Meretoja V, Kasper FK, Mikos A. TGF-β3-induced chondrogenesis in co-cultures of chondrocytes and mesenchymal stem cells on biodegradable scaffolds. Biomaterials 2014;35:123–32.
32. Khor B, Gagnon JD, Goel G, Roche MI, Conway KL, Tran K, *et al*. The kinase DYRK1A reciprocally regulates the differentiation of Th17 and regulatory T cells. Elife 2015;4.
33. Haczku A, Alexander A, Brown P, Assoufi B, Li B, Kay AB, *et al*. The effect of dexamethasone, cyclosporine, and rapamycin on T-lymphocyte proliferation in vitro: comparison of cells from patients with glucocorticoid-sensitive and glucocorticoid-resistant chronic asthma. J Allergy Clin Immunol 1994;93:510–9.
34. Ferron GM, Pyszczynski NA, Jusko WJ. Gender-related assessment of cyclosporine/prednisolone/sirolimus interactions in three human lymphocyte proliferation assays. Transplantation 1998;65:1203–9.
35. Jang J, Jung Y, Kim Y, Jho E-H, Yoon Y. LPS-induced inflammatory response is suppressed by Wnt inhibitors, Dickkopf-1 and LGK974. Sci Rep 2017;7:41612.
36. Malfait AM, Little CB, McDougall JJ. A commentary on modelling osteoarthritis pain in small animals. Osteoarthritis Cartilage 2013;21:1316–26.
37. Takahashi I, Matsuzaki T, Kuroki H, Hoso M. Induction of osteoarthritis by injecting monosodium iodoacetate into the patellofemoral joint of an experimental rat model. PLoS One 2018;13:1–15.
38. Glasson SS, Chambers MG, Van Den Berg WB, Little CB. The OARSI histopathology initiative - recommendations for histological assessments of osteoarthritis in the mouse. Osteoarthritis Cartilage 2010;18(Suppl 3):S17–23.
39. Lories RJ, Corr M, Lane NE. To Wnt or not to Wnt: the bone and joint health dilemma. Nat Rev Rheumatol 2013;9:328–39.
40. Gao C, Xiao G, Hu J. Regulation of Wnt/β-catenin signaling by posttranslational modifications. Cell Biosci 2014;4:13.
41. Verheyen EM, Gottardi CJ. Regulation of Wnt/beta-catenin signaling by protein kinases. Dev Dynam 2010;239:34–44.
42. Ring A, Kim Y-M, Kahn M. Wnt/catenin signaling in adult stem cell physiology and disease. Stem Cell Rev 2014;10:512–25.
43. Lu B, Green BA, Farr JM, Lopes FCM, Van Raay TJ. Wnt drug discovery: weaving through the screens, patents and clinical trials. Cancers (Basel). 2016;8.
44. Kahn M. Can we safely target the WNT pathway? Nat Rev Drug Discov 2014;13:513–32.
45. Nalesso G, Thomas BL, Sherwood JC, Yu J, Addimanda O, Eldridge SE, *et al*. WNT16 antagonises excessive canonical WNT activation and protects cartilage in osteoarthritis. Ann Rheum Dis 2016;0:1–9.
46. Chun J-S, Oh H, Yang S, Park M. Wnt signaling in cartilage development and degeneration. BMB Rep 2008;41:485–94.
47. Funnell T, Tasaki S, Oloumi A, Araki S, Kong E, Yap D, *et al*. CLK-dependent exon recognition and conjoined gene formation revealed with a novel small molecule inhibitor. Nat Commun 2017;8:7.
48. Isken O, Maquat LE. The multiple lives of NMD factors: balancing roles in gene and genome regulation. Nat Rev Genet 2008;9:699–712.
49. Monteagudo S, Cornelis FMF, Aznar-Lopez C, Yibmantasiri P, Guns L-A, Carmeliet P, *et al*. DOT1L safeguards cartilage homeostasis and protects against osteoarthritis. Nat Commun 2017;8:15889.
50. Zhou Y, Song T, Peng J, Zhou Z, Wei H, Rui Z, *et al*. SIRT1 suppresses adipogenesis by activating Wntβ-catenin signaling in vivo and in vitro. Oncotarget 2016;7.